



Numerical study of the non-linear time fractional Klein-Gordon equation using the Pseudo-spectral Method

Soheila Mirzaei and Ali Shokri*

Department of Mathematics, Faculty of Sciences, University of Zanjan, Zanjan, Iran.

Abstract

This paper presents a numerical scheme for solving the non-linear time fractional Klein-Gordon equation. To approximate spatial derivatives, we employ the pseudo-spectral method based on Lagrange polynomials at Chebyshev points, while using the finite difference method for time discretization. Our analysis demonstrates that this scheme is unconditionally stable, with a time convergence order of $\mathcal{O}(3 - \alpha)$. Additionally, we provide numerical results in one, two, and three dimensions, highlighting the high accuracy of our approach. The significance of our proposed method lies in its ability to efficiently and accurately address the non-linear time fractional Klein-Gordon equation. Furthermore, our numerical outcomes validate the effectiveness of this scheme across different dimensions.

Keywords. Fractional derivatives, Non-linear Klein-Gordon equation, Pseudo-spectral method, Lagrange polynomials, Finite difference scheme.

2010 Mathematics Subject Classification. 65M70, 35R11, 65M06.

1. INTRODUCTION

During the last few decades, fractional differential equations have shown a significant role in various fields of engineering and science. Also, these equations have been used for several models containing signal processing, diffusion models, traffic and fluid flow model [1, 16, 19, 27]. Non-integer calculus has attention in several fields of mathematical biology and electro-chemistry [31] and also in different physical phenomena including relative stress and strain for elastic materials, viscoelastic materials, and Hooks law [8, 21, 27].

One of the most widely used fractional equations is the non-linear time fractional Klein-Gordon (TFKG) equation, whose general form is

$$\zeta^{\alpha-1} \frac{\partial^\alpha u}{\partial t^\alpha} + \gamma \frac{\partial u}{\partial t} + \beta u = \Delta u + \lambda u^3 + \zeta^{\alpha-1} f, \quad (1.1)$$

in the finite domain $\Omega = [a, b]^d$, $d = 1, 2, 3$ and $0 < t < T$ with the initial conditions

$$u(x, 0) = \varphi_1(x), \quad \frac{\partial u(x, 0)}{\partial t} = \varphi_2(x), \quad x \in \Omega, \quad (1.2)$$

and boundary conditions

$$u(a, t) = \psi_1(t), \quad u(b, t) = \psi_2(t), \quad t \in [0, T]. \quad (1.3)$$

The f in (1.1) is a given smooth function in $\Omega \times (0, T)$ and functions $\varphi_1, \varphi_2, \psi_1$, and ψ_2 in initial and boundary conditions are smooth functions in their domains. In addition, coefficients ζ, γ, β , and λ are constant.

Note that if $\lambda \neq 0$, we have the non-linear TFKG equation, but for $\lambda = 0$, we have the linear TFKG equation. For $\alpha = 1$, Equation (1.1) is reduced to the standard KG equation.

Received: 25 October 2023; Accepted: 25 June 2024.

* Corresponding author. Email: a.shokri@znu.ac.ir, shokri.a@gmail.com.

The Δ in (1.1) is the Laplace space operator, and $\frac{\partial^\alpha u}{\partial t^\alpha}$ denotes the Caputo type fractional derivative of order α that defines as

$$\frac{\partial^\alpha u(x, t)}{\partial t^\alpha} = \frac{1}{\Gamma(2-\alpha)} \int_0^t \frac{\partial^2 u(x, s)}{\partial t^2} (t-s)^{1-\alpha} ds, \quad 1 < \alpha < 2, \quad (1.4)$$

where $\Gamma(\cdot)$ is the Gamma function [8, 27].

The physical significance of each term in the non-linear TFKG Equation (1.1) is as follows:

- $\zeta^{\alpha-1} \frac{\partial^\alpha u}{\partial t^\alpha}$: This term represents the fractional derivative of the field variable u with respect to time t . The parameter ζ is related to the fractional order α and characterizes the memory effect in the system. Physically, it accounts for the memory-dependent behavior of the field, where past values of u influence its current behavior. The fractional derivative captures non-local effects.
- $\gamma \frac{\partial u}{\partial t}$: The term involving γ represents the damping or dissipation effect. It describes how energy dissipates from the system due to friction, viscosity, or other dissipative processes. Larger values of γ lead to faster decay of oscillations in the field u .
- βu : The parameter β is associated with the mass of the field. It represents the inertia or resistance to changes in motion. Physically, this term contributes to the field's oscillatory behavior and its response to external forces.
- Δu : The Laplacian operator Δ acts on the field u and represents spatial variations. It captures how the field evolves in space. This term accounts for dispersion and wave propagation effects. It is related to the curvature of the field profile.
- λu^3 : The nonlinearity in the equation arises from this cubic term. The parameter λ characterizes the strength of the nonlinearity. Physically, this term represents self-interaction or self-coupling of the field. It leads to phenomena such as solitons or localized wave packets.
- $\zeta^{\alpha-1} f$: The function f represents external forcing or sources. The parameter ζ is again related to the fractional order α . This term accounts for any external influences acting on the field u , such as external fields, boundary conditions, or driving forces.

The KG equation appears in many modeling of physical phenomena such as superconductors, dislocations in crystals, and the motion of the pendulum [13, 33, 35, 41]. Another application of this equation can be mentioned as a constitutive equation to obtain a quasi-heterogeneous model for introducing the problem of air diffusion reaction of a disordered porous medium [14, 32]. Özkan and Özkan [26] derived exact soliton solutions for the space time-fractional Klein-Gordon equation, incorporating cubic nonlinearities through the solitary wave ansatz method. Additionally, they demonstrated some of these solutions using computer simulations.

In paper [33], the authors implemented a high-order finite difference scheme for the two-dimensional FKG equation with the Neumann boundary condition. Mohebi et al. [22] used the compact differential method of order $\mathcal{O}(h^4 + \tau^{3-\alpha})$ for the FKG equation with $1 < \alpha < 2$.

Hosseini et al. in [18] solved the TFKG equation with quadratic and cubic non-linearities via the modified Kudryashv method. To solve the KG equation in the Cantor set, Komar et al. [7] used a computational scheme using fractional Sumudu transformation and homotopy perturbation technique. In [34], Vong and Wang introduced a high-order finite difference method for a non-linear FKG equation. Yin et al. in [37] used a coupled method of Laplace transform and Legendre wavelets (LLW) for the approximate solutions of the non-linear KG equation. Nagy [24] considered the Sinc-Chebyshev collocation method to solve the non-linear FKG equation.

So far, many numerical methods have been proposed for solving partial differential equations. These methods are divided into global and local groups. The basis of spectral and pseudo-spectral methods is global approximations. The use of spectral methods in solving differential equations during the 1970s revealed the superiority of these methods in simulating issues with a regular domain. If the problem data is smooth, spectral methods are the best tools. They can also get high accuracy and usually require less computer memory [4].

Now we delve into the distinctive features of our proposed method for solving the non-linear time fractional Klein-Gordon equation. Our approach stands out in several key ways:



Pseudo-Spectral Method: Unlike conventional methods commonly employed in the literature, we introduce a novel pseudo-spectral approach. By leveraging spectral techniques, our method achieves high accuracy and stability. The choice of pseudo-spectral basis functions allows us to efficiently handle non-linearities and fractional derivatives, which are inherent in the Klein-Gordon equation.

Lagrange Polynomials on Chebyshev Points: Our selection of Lagrange polynomials as basis functions is a departure from existing works. While other methods often rely on orthogonal polynomials, we harness the unique properties of Chebyshev points. The use of Chebyshev points enhances the convergence rate and computational efficiency of our method, especially when dealing with irregular domains or non-uniform grids.

Demonstrated Effectiveness: To validate our approach, we present three illustrative examples in different dimensions. These examples showcase the methods robustness and accuracy across various scenarios. By comparing our results with those obtained using traditional methods, we highlight the superior performance of our proposed approach.

Unconditional Stability: Rigorous stability analysis forms an integral part of our contribution. We prove that our method remains stable under all conditions, regardless of the problem parameters. This stability property ensures reliable numerical solutions even in challenging scenarios.

Exponential Accuracy: Perhaps the most compelling feature of our method is its exponential accuracy. Unlike linear convergence observed in some existing methods, our approach exhibits rapid convergence rates. Researchers seeking highly accurate solutions will find our method particularly advantageous.

In the following, we review some recent works in which spectral and pseudo-spectral methods have been used on fractional PDEs. In the work by Youssri [38], the spectral solutions for the nonlinear fractional Klein-Gordon equation were obtained using both the typical collocation method and the tau method. To achieve this, a novel operational matrix of fractional derivatives based on Fibonacci polynomials was introduced. The authors in [40], introduced a new numerical technique called the Rectified Chebyshev Petrov-Galerkin Procedure. This method addresses the time-fractional heat conduction equation with nonlocal conditions in the temporal domain. By extending the classical Petrov-Galerkin method, it efficiently handles the fractional temporal derivatives involved. In their research, Youssri and Atta [39] developed an explicit modal numerical solver using the spectral PetrovGalerkin method. They combined shifted Chebyshev polynomial basis functions to handle the nonlinear time-fractional Burgers-type partial differential equation in the Caputo sense.

Moustafa et al. [23] suggested using a potent spectral approach to solve the time-fractional diffusion equation. In [15] Hafez and colleagues utilized a rational Jacobi collocation technique to handle linear time-fractional sub-diffusion and reaction sub-diffusion equations. The semi-analytic approximation solution represents spatial and temporal variables using a series of rational Jacobi polynomials. This approach simplifies the problem and enables efficient computation of the solution coefficients. In their research, Taherkhani and colleagues [29] introduced a pseudospectral method that relies on Sinc operational matrices to solve nonlinear time-fractional Klein-Gordon and sine-Gordon equations. They discretized the Caputo time-fractional derivative using a finite difference scheme, while approximating spatial derivatives with the Sinc method. Another study by different authors [25] proposed a numerical approach based on the CrankNicolson scheme and the Tau method for solving the nonlinear KleinGordon equation. By reducing the nonlinear KleinGordon equation to a system of ordinary differential equations using the CrankNicolson scheme, they then employed the Tau method, leveraging interpolating scaling functions and the operational matrix of derivatives.

This paper consists of six sections. In the second section, we explain the method of discretizing the time derivatives. In the third section, we introduce the pseudo-spectral method and then implement it on the TFKG equation, and we obtain the final discretized equation. In the next section we prove that the presented scheme is unconditionally stable. In the fifth section, we show the effectiveness of the prescribed method by implementing three examples in the different dimensions. And finally, we give the conclusion of this paper.

2. TIME DISCRETIZATION SCHEME

Some discretization methods are chosen because of their ease of implementation. Moreover, certain discretization methods provide high precision in representing continuous data, which is crucial for accurate modeling and analysis. To discretize the time derivatives, for positive integer number N , suppose $t_k = k\eta$ ($k = 0, 1, \dots, N$) be the time steps



with the step size $\eta = T/N$. Also, let $u^k = u(\mathbf{x}, t_k)$ be a grid function on $\Omega \times (0, T)$. We introduce the following symbols:

$$\begin{aligned} u^{k-1/2} &= \frac{1}{2} (u^k + u^{k-1}), & \delta_t u^{k-1/2} &= \frac{1}{\eta} (u^k - u^{k-1}), \\ \delta_x^2 u^{k-1/2} &= \frac{1}{2} (\delta_x^2 u^k + \delta_x^2 u^{k-1}). \end{aligned} \quad (2.1)$$

where $u^{k-1/2}$ represents the average of u at the points (\mathbf{x}, t_k) and (\mathbf{x}, t_{k-1}) , $\delta_t u^{k-1/2}$ denotes the difference quotient of u based on these two points, and $\delta_x^2 u^{k-1/2}$ corresponds to the average of the second-order difference quotient at these points. We approximate the fractional time derivative in Equation (1.1) using the following difference scheme [28]

$$\frac{\partial^\alpha u^k}{\partial t^\alpha} \simeq \frac{1}{\eta \Gamma(2-\alpha)} \left[\mu_0 \delta_t u^{k-1/2} - \sum_{i=1}^{k-1} (\mu_{k-i-1} - \mu_{k-i}) \delta_t u^{i-1/2} - \mu_{k-1} \phi \right], \quad (2.2)$$

where $\phi = \frac{\partial u}{\partial t} \Big|_{t=0}$. The coefficients μ_j are obtained as follows

$$\mu_j = \int_{t_j}^{t_{j+1}} \frac{dt}{t^{\alpha-1}} = \frac{\eta^{2-\alpha}}{2-\alpha} [(j+1)^{2-\alpha} - (j)^{2-\alpha}], \quad j \geq 0. \quad (2.3)$$

To express the error of this approximation, we take some lemmas from reference [28]. To see the proof of these lemmas, you can refer to this reference.

Lemma 2.1. [28] For positive integer number $n \geq 1$ such that $t_k = k\eta$ ($k = 0, 1, \dots, n$), we have

$$\begin{aligned} 0 &\leq \sum_{j=1}^n \int_{t_{j-1}}^{t_j} \left\{ (t_n - t)^{2-\alpha} - \left[\frac{t - t_{j-1}}{\eta} (t_n - t_j)^{2-\alpha} + \frac{t_j - t}{\eta} (t_n - t_{j-1})^{2-\alpha} \right] \right\} dt \\ &\leq \left[\frac{2-\alpha}{12} + \frac{2^{3-\alpha}}{3-\alpha} - (1 + 2^{1-\alpha}) \right] \eta^{3-\alpha}. \end{aligned}$$

Lemma 2.2. [28] Let $h(t) \in C^2[0, t_k]$, then we have

$$\begin{aligned} &\left| \int_0^{t_k} h'(t) \frac{dt}{(t_k - t)^{\alpha-1}} - \sum_{j=1}^k \frac{h(t_j) - h(t_{j-1})}{\eta} \int_{t_{j-1}}^{t_j} \frac{dt}{(t_k - t)^{\alpha-1}} \right| \\ &\leq \frac{1}{2-\alpha} \left[\frac{2-\alpha}{12} + \frac{2^{3-\alpha}}{3-\alpha} - (1 + 2^{1-\alpha}) \right] \max_{1 \leq t \leq t_k} |h''(t)| \eta^{3-\alpha}. \end{aligned}$$

Lemma 2.3. [28] Let $h(t) \in C^2[0, t_k]$, then we have

$$\begin{aligned} &\left| \int_0^{t_k} h'(t) \frac{dt}{(t_k - t)^{\alpha-1}} - \frac{1}{\eta} \left[\mu_0 h(t_k) - \sum_{j=1}^{k-1} (\mu_{k-j-1} - \mu_{k-j}) h(t_j) - \mu_{k-1} h(t_0) \right] \right| \\ &\leq \frac{1}{2-\alpha} \left[\frac{2-\alpha}{12} + \frac{2^{3-\alpha}}{3-\alpha} - (1 + 2^{1-\alpha}) \right] \max_{1 \leq t \leq t_k} |h''(t)| \eta^{3-\alpha}. \end{aligned}$$

where μ_j is defined in (2.3) and $1 < \alpha < 2$.

Therefore, according to the Lemma 2.3, the accuracy of approximation (2.2) is of order $\eta^{3-\alpha}$. Now, using the approximations (2.1)-(2.2), we obtain the time discrete scheme of TFKG Equation (1.1) as

$$\begin{aligned} &\frac{\zeta^{\alpha-1}}{\eta \Gamma(2-\alpha)} \left[\mu_0 \delta_t u^{k-1/2} - \sum_{i=1}^{k-1} (\mu_{k-i-1} - \mu_{k-i}) \delta_t u^{i-1/2} - \mu_{k-1} \phi \right] + \gamma \delta_t u^{k-1/2} \\ &+ \beta u^{k-1/2} = \delta_x^2 u^{k-1/2} + \delta_y^2 u^{k-1/2} + \lambda (u^{k-1})^3 + \zeta^{\alpha-1} f^{k-1/2}, \end{aligned} \quad (2.4)$$



for $k = 1, 2, \dots, N$. It is necessary to explain that, according to the second-order accuracy of the Crank-Nicolson method in approximating the ordinary derivative with respect to time and the $\eta^{3-\alpha}$ th-order accuracy of the fractional derivative approximation (2.2), the discretization (2.4) has an accuracy of at least 2 with respect to the time variable. Additionally, to avoid encountering a non-linear system, the term u^3 has been retained in the t_{k-1} time step. Consequently, the final system resulting from the discretization will be linear.

In the next section, we will discuss how to apply the pseudo-spectral method to the Equation (2.4).

3. THE PSEUDO-SPECTRAL METHOD

In this section, we give a brief explanation of the pseudo-spectral methods. The pseudo-spectral method is a robust numerical technique used for solving partial differential equations (PDEs) and ordinary differential equations (ODEs). Here are the key points:

- Pseudo-spectral methods excel when precision is crucial. They outperform finite difference or finite element methods.
- While finite methods typically achieve an accuracy of 2 or 3, spectral methods can reach an impressive level of 10.
- Pseudo-spectral methods are particularly effective when dealing with smooth data (e.g., continuous functions).
- They shine in problems where the solution exhibits regular behavior.
- Pseudo-spectral methods work well on simple domains.
- Their performance is optimized when the problem domain has straightforward geometric boundaries.
- Unlike some other methods, pseudo-spectral techniques require less computer memory.
- This efficiency makes them attractive for large-scale simulations and computationally intensive tasks.

In summary, pseudo-spectral methods combine the benefits of spectral methods with additional pseudo-spectral bases, enabling accurate solutions while maintaining computational efficiency (for more information about the spectral and pseudo-spectral methods see [4]).

In pseudo-spectral methods, choosing the bases of the approximation space is very important. In this work, we present a suitable approximation of the solution in terms of Lagrange polynomials. Lagrange polynomials provide precise interpolation at the specified data points. Unlike some other basis functions, they pass through all data points, ensuring accurate representation. Additionally, calculating Lagrange coefficients is straightforward. Furthermore, the Lagrange approach diagonalizes the coefficient problem, resulting in computational efficiency. Moreover, Lagrange interpolation remains effective even when the data points are not equally spaced. In summary, Lagrange polynomials strike a balance between accuracy, ease of computation, and versatility, making them a valuable choice for interpolation tasks.

Note that we use the pseudo-spectral method only to discretize the spatial variable. Also, we describe the implementation of the method for the two-dimensional case. The execution steps are similar for one-dimensional and three-dimensional modes.

Suppose $\Omega \subseteq \mathbb{R}^2$ is a bounded domain and n_p is a positive integer. Chebyshev polynomials are a sequence of orthogonal polynomials defined on the interval $[-1, 1]$. They have several useful properties for numerical computations, including minimizing the Runge phenomenon. The roots of Chebyshev polynomials are known as Chebyshev points, which are defined as follows:

$$x_{ij} = (\cos(i\pi/n_p), \cos(j\pi/n_p)), \quad i, j = 0, 1, \dots, n_p. \quad (3.1)$$

To approximate the unknown functions, we want to write them as linear combinations of basis functions. To this end, we consider the following Lagrange polynomials as basis functions:

$$l_{ij}(x, y) = l_i(x)l_j(y), \quad i, j = 0, 1, \dots, n_p, \quad (3.2)$$

where

$$l_i(x) = \prod_{\substack{k=0 \\ k \neq i}}^{n_p} \left(\frac{x - x_k}{x_i - x_k} \right), \quad i = 0, 1, \dots, n_p.$$



Note that $\ell_i(x) \in \mathbb{P}_{n_p}$ (polynomials of degree $\leq n_p$) and satisfy in the Kronecker Delta property. We consider the solution of (1.1) and the right-hand side function f as a linear combination of Lagrange polynomials as

$$u_{n_p}(x, y, t) = \sum_{i,j=1}^{n_p-1} u_{ij}(t) \ell_{ij}(x, y), \quad u_{ij}(t) := u(x_{ij}, t), \quad (3.3)$$

$$f_{n_p}(x, y, t) = \sum_{i,j=1}^{n_p-1} f_{ij}(t) \ell_{ij}(x, y), \quad f_{ij}(t) := f(x_{ij}, t). \quad (3.4)$$

To compute derivatives, we utilize differentiation matrices based on Chebyshev points (3.1). These matrices approximate derivatives by evaluating the derivative at Chebyshev points. Now, we could find the second-order derivatives of $\ell_{ij}(\cdot)$ concerning x and y in Chebyshev points (3.1) as

$$\begin{aligned} \frac{\partial^2}{\partial x^2} \ell_{ij}(x_{rs}) &= \ell_i''(x_r) \ell_j(y_s) = \left[D_{n_p}^2 \right]_{ri} \delta_{js}, \quad r, s = 0, 1, \dots, n_p, \\ \frac{\partial^2}{\partial y^2} \ell_{ij}(x_{rs}) &= \ell_i(x_r) \ell_j''(y_s) = \delta_{ri} \left[D_{n_p}^2 \right]_{js}, \quad r, s = 0, 1, \dots, n_p, \end{aligned}$$

where $D_{n_p}^2$ is the second-order derivative matrix in Chebyshev points. Furthermore, the discrete Laplacian is obtained as

$$\Delta \ell_{ij}(x_{rs}) = I_{n_p} \otimes D_{n_p}^2 + D_{n_p}^2 \otimes I_{n_p},$$

where the symbol \otimes represents the Kronecker tensor product of two matrices [17]. Putting these relations in Equation (2.4), we get:

$$\begin{aligned} &\frac{\zeta^{\alpha-1}}{\eta \Gamma(2-\alpha)} \left[\mu_0 \delta_t u_{n_p}^{k-1/2} - \sum_{i=1}^{k-1} (\mu_{k-i-1} - \mu_{k-i}) \delta_t u_{n_p}^{i-1/2} - \mu_{k-1} \phi \right] + \gamma \delta_t u_{n_p}^{k-1/2} \\ &+ \beta u_{n_p}^{k-1/2} = \sum_{i,j=1}^{n_p-1} \left(\left[D_{n_p}^2 \right]_{ri} \delta_{js} \right) u_{rs}^{k-1/2} + \sum_{i,j=1}^{n_p-1} \left(\delta_{ri} \left[D_{n_p}^2 \right]_{js} \right) u_{rs}^{k-1/2} \\ &+ \lambda \left(u_{n_p}^{k-1} \right)^3 + \zeta^{\alpha-1} \sum_{i,j=1}^{n_p-1} f_{rs}^{k-1/2}, \quad r, s = 0, 1, \dots, n_p. \end{aligned} \quad (3.5)$$

Also, note that for $i = 0, n_p$ and $j = 0, n_p$, $u(x_{ij}, t)$ is already known from the homogeneous boundary conditions (1.3). For simplicity, we write the Equation (3.5) in the matrix form:

$$\begin{aligned} &\nu \mu_0 U_{n_p}^k + \frac{\gamma}{\eta} U_{n_p}^k + \frac{\beta}{2} U_{n_p}^k - \frac{1}{2} \sum_{i,j=1}^{n_p-1} \left(\left[D_{n_p}^2 \right]_{ri} \delta_{js} + \delta_{ri} \left[D_{n_p}^2 \right]_{js} \right) U_{rs}^k \\ &= \nu \mu_0 U_{n_p}^{k-1} + \frac{\gamma}{\eta} U_{n_p}^{k-1} - \frac{\beta}{2} U_{n_p}^{k-1} + \frac{1}{2} \sum_{i,j=1}^{n_p-1} \left(\left[D_{n_p}^2 \right]_{ri} \delta_{js} + \delta_{ri} \left[D_{n_p}^2 \right]_{js} \right) U_{rs}^{k-1} \\ &+ \nu \sum_{i=1}^{k-1} (\mu_{k-i-1} - \mu_{k-i}) \delta_t U_{n_p}^{i-1/2} + \nu \mu_{k-1} U^0 + \lambda \left(U_{n_p}^{k-1} \right)^3 + \zeta^{\alpha-1} \sum_{i,j=1}^{n_p-1} f_{rs}^{k-1/2}, \end{aligned} \quad (3.6)$$

where $\nu = \frac{\zeta^{\alpha-1}}{\eta^2 \Gamma(2-\alpha)}$.

4. STABILITY

Stability ensures that the numerical solution remains bounded over time. Unstable methods can lead to exponential growth of errors, rendering the results unreliable. On the other hand, stable methods respect physical constraints. For



example, in fluid flow simulations, stable methods prevent unphysical negative densities or temperatures. Therefore, numerical stability significantly impacts the reliability, accuracy, and efficiency of PDE solvers. Choosing stable methods ensures robust simulations and meaningful results.

In this section, by presenting a theorem along with its proof, we show that the above method is unconditionally stable. For this purpose, for the ease of proving the stability, we define the following operator:

$$\mathcal{P} \left(u^{n-\frac{1}{2}}, \phi \right) = \mu_0 u^{n-1/2} - \sum_{k=1}^{n-1} (\mu_{n-k-1} - \mu_{n-k}) u^{k-1/2} - \mu_{n-1} \phi. \tag{4.1}$$

Using this operator and putting $\zeta = 1$, we can write the time discrete scheme (2.4) as

$$\begin{cases} \frac{1}{\eta\Gamma(2-\alpha)} \mathcal{P} \left(\delta_t U^{n-\frac{1}{2}}, \phi \right) + \gamma \delta_t U^{n-\frac{1}{2}} + \beta U^{n-\frac{1}{2}} = \Delta U^{n-\frac{1}{2}} + \dots \\ \dots + \lambda (U^{n-1})^3 + f^{n-\frac{1}{2}}, & x \in \Omega, \quad n \geq 1, \\ U^n = 0, & x \in \partial\Omega. \end{cases} \tag{4.2}$$

Lemma 4.1. [22] For any $\Phi = \{\Phi_1, \Phi_2, \dots\}$ and ϕ , we obtain

$$\sum_{n=1}^N \mathcal{P}(\Phi_n, \phi) \Phi_n \geq \frac{t_N^{1-\alpha}}{2} \eta \sum_{n=1}^N \Phi_n^2 - \frac{t_N^{2-\alpha}}{2(2-\alpha)} \phi, \quad N = 1, 2, \dots$$

To prove the stability of the method, we present the following theorem.

Theorem 4.2. Assume $U^n \in H_0^1(\Omega)$ and $\phi = \frac{\partial u}{\partial t}|_{t=0}$. Then the time discrete scheme (4.2) is unconditionally stable and we have the following inequality

$$\|U^n\|_{L^2(\Omega)} \leq \mathcal{C},$$

where \mathcal{C} is a positive constant.

Proof. By multiplying the sides of the Equation (4.2) by $\delta_t U^{n-\frac{1}{2}}$ and taking the integral over the Ω , we have

$$\begin{aligned} & \frac{1}{\eta\Gamma(2-\alpha)} \left\{ \mu_0 (\delta_t U^{n-\frac{1}{2}}, \delta_t U^{n-\frac{1}{2}}) - \sum_{k=1}^{n-1} (\mu_{n-k-1} - \mu_{n-k}) (\delta_t U^{k-\frac{1}{2}}, \delta_t U^{n-\frac{1}{2}}) \right. \\ & \quad \left. - \mu_{n-1} (\phi, \delta_t U^{n-\frac{1}{2}}) \right\} + \gamma (\delta_t U^{n-\frac{1}{2}}, \delta_t U^{n-\frac{1}{2}}) + \beta (U^{n-\frac{1}{2}}, \delta_t U^{n-\frac{1}{2}}) \\ & = (\nabla^2 U^{n-\frac{1}{2}}, \delta_t U^{n-\frac{1}{2}}) + \lambda ((U^{n-1})^3, \delta_t U^{n-\frac{1}{2}}) + (f^{n-\frac{1}{2}}, \delta_t U^{n-\frac{1}{2}}). \end{aligned} \tag{4.3}$$

Using the $L^2(\Omega)$ -norm we obtain

$$\begin{aligned} & \frac{1}{\eta\Gamma(2-\alpha)} \left\{ \mu_0 \|\delta_t U^{n-\frac{1}{2}}\|_{L^2(\Omega)}^2 - \sum_{k=1}^{n-1} (\mu_{n-k-1} - \mu_{n-k}) \|\delta_t U^{k-\frac{1}{2}}\|_{L^2(\Omega)} \|\delta_t U^{n-\frac{1}{2}}\|_{L^2(\Omega)} \right. \\ & \quad \left. - \mu_{n-1} \|\phi\|_{L^2(\Omega)} \|\delta_t U^{n-\frac{1}{2}}\|_{L^2(\Omega)} \right\} + \gamma \|\delta_t U^{n-\frac{1}{2}}\|_{L^2(\Omega)}^2 + \beta (U^{n-\frac{1}{2}}, \delta_t U^{n-\frac{1}{2}}) \\ & \leq -(\nabla U^{n-\frac{1}{2}}, \nabla \delta_t U^{n-\frac{1}{2}}) + \lambda ((U^{n-1})^3, \delta_t U^{n-\frac{1}{2}}) + (f^{n-\frac{1}{2}}, \delta_t U^{n-\frac{1}{2}}). \end{aligned} \tag{4.4}$$

Also, we have

$$\begin{aligned} (U^{n-\frac{1}{2}}, \delta_t U^{n-\frac{1}{2}}) & = \int_{\Omega} (U^{n-\frac{1}{2}}) (\delta_t U^{n-\frac{1}{2}}) d\Omega \\ & = \int_{\Omega} \left(\frac{U^n + U^{n-1}}{2} \right) \left(\frac{U^n - U^{n-1}}{\eta} \right) d\Omega \\ & = \frac{1}{2\eta} \left\{ \|U^n\|_{L^2(\Omega)}^2 - \|U^{n-1}\|_{L^2(\Omega)}^2 \right\}, \end{aligned} \tag{4.5}$$



and

$$\begin{aligned}
(\nabla U^{n-\frac{1}{2}}, \nabla \delta_t U^{n-\frac{1}{2}}) &= \int_{\Omega} (\nabla U^{n-\frac{1}{2}})(\nabla \delta_t U^{n-\frac{1}{2}}) d\Omega \\
&= \int_{\Omega} \left(\frac{\nabla U^n + \nabla U^{n-1}}{2} \right) \left(\frac{\nabla U^n - \nabla U^{n-1}}{\eta} \right) d\Omega \\
&= \frac{1}{2\eta} \left\{ \|\nabla U^n\|_{L^2(\Omega)}^2 - \|\nabla U^{n-1}\|_{L^2(\Omega)}^2 \right\}.
\end{aligned} \tag{4.6}$$

Assuming relation (4.4) for $n = 1, \dots, m$ and using relations (4.5)-(4.6), we have the following inequality

$$\begin{aligned}
\frac{1}{\eta\Gamma(2-\alpha)} \sum_{n=1}^m \left\{ \mu_0 \|\delta_t U^{n-\frac{1}{2}}\|_{L^2(\Omega)} - \sum_{k=1}^{n-1} (\mu_{n-k-1} - \mu_{n-k}) \|\delta_t U^{k-\frac{1}{2}}\|_{L^2(\Omega)} \right. \\
\left. - \mu_{n-1} \|\phi\|_{L^2(\Omega)} \right\} \|\delta_t U^{n-\frac{1}{2}}\|_{L^2(\Omega)} + \gamma \sum_{n=1}^m \|\delta_t U^{n-\frac{1}{2}}\|_{L^2(\Omega)}^2 \\
+ \frac{\beta}{2\eta} \left\{ \|U^m\|_{L^2(\Omega)}^2 - \|U^0\|_{L^2(\Omega)}^2 \right\} + \frac{1}{2\eta} \left\{ \|\nabla U^m\|_{L^2(\Omega)}^2 - \|\nabla U^0\|_{L^2(\Omega)}^2 \right\} \\
\leq \sum_{n=1}^m \left\{ \lambda ((U^{n-1})^3, \delta_t U^{n-\frac{1}{2}}) + (f^{n-\frac{1}{2}}, \delta_t U^{n-\frac{1}{2}}) \right\}.
\end{aligned} \tag{4.7}$$

By setting $\Phi_n = \|\delta_t U^{n-\frac{1}{2}}\|_{L^2(\Omega)}$ and $\phi = \|\phi\|_{L^2(\Omega)}$ in Lemma 4.1, we find

$$\begin{aligned}
\frac{t_m^{1-\alpha}}{2\Gamma(2-\alpha)} \sum_{n=1}^m \|\delta_t U^{n-\frac{1}{2}}\|_{L^2(\Omega)}^2 - \frac{t_m^{2-\alpha}}{2\eta(2-\alpha)\Gamma(2-\alpha)} \|\phi\|_{L^2(\Omega)}^2 + \gamma \sum_{n=1}^m \|\delta_t U^{n-\frac{1}{2}}\|_{L^2(\Omega)}^2 \\
+ \frac{\beta}{2\eta} \left\{ \|U^m\|_{L^2(\Omega)}^2 - \|U^0\|_{L^2(\Omega)}^2 \right\} + \frac{1}{2\eta} \left\{ \|\nabla U^m\|_{L^2(\Omega)}^2 - \|\nabla U^0\|_{L^2(\Omega)}^2 \right\} \\
\leq \lambda \sum_{n=1}^m ((U^{n-1})^3, \delta_t U^{n-\frac{1}{2}}) + \sum_{n=1}^m (f^{n-\frac{1}{2}}, \delta_t U^{n-\frac{1}{2}}).
\end{aligned} \tag{4.8}$$

Now, using the inequality

$$pq \leq \frac{1}{2\theta^2} p^2 + \frac{\theta^2}{2} q^2, \quad \forall \theta \neq 0, \tag{4.9}$$

to the sentences on the right side of inequality (4.8) we obtain

$$\begin{aligned}
\frac{(1-\lambda)t_m^{1-\alpha} + 2\gamma\Gamma(2-\alpha)}{2\Gamma(2-\alpha)} \sum_{n=1}^m \|\delta_t U^{n-\frac{1}{2}}\|_{L^2(\Omega)}^2 - \frac{t_m^{2-\alpha}}{2\eta(2-\alpha)\Gamma(2-\alpha)} \|\phi\|_{L^2(\Omega)}^2 \\
+ \frac{\beta}{2\eta} \left\{ \|U^m\|_{L^2(\Omega)}^2 - \|U^0\|_{L^2(\Omega)}^2 \right\} + \frac{1}{2\eta} \left\{ \|\nabla U^m\|_{L^2(\Omega)}^2 - \|\nabla U^0\|_{L^2(\Omega)}^2 \right\} \\
\leq \frac{\lambda\Gamma(2-\alpha)}{2t_m^{1-\alpha}} \sum_{n=1}^m \|(U^{n-1})^3\|_{L^2(\Omega)}^2 + \frac{(1-\lambda)t_m^{1-\alpha} + 2\gamma\Gamma(2-\alpha)}{2\Gamma(2-\alpha)} \sum_{n=1}^m \|\delta_t U^{n-\frac{1}{2}}\|_{L^2(\Omega)}^2 \\
+ \frac{\Gamma(2-\alpha)}{(1-\lambda)t_m^{1-\alpha} + 2\gamma\Gamma(2-\alpha)} \sum_{n=1}^m \|f^{n-\frac{1}{2}}\|_{L^2(\Omega)}^2.
\end{aligned} \tag{4.10}$$



By simplifying, changing the sigmas upper index from m to n , multiplying both sides of (4.10) into 2η , and considering $\phi = 0$, we have

$$\beta \left\{ \|U^n\|_{L^2(\Omega)}^2 - \|U^0\|_{L^2(\Omega)}^2 \right\} + \|\nabla U^n\|_{L^2(\Omega)}^2 \leq \frac{\eta\lambda\Gamma(2-\alpha)}{t_n^{1-\alpha}} \sum_{j=1}^n \|(U^{n-1})^3\|_{L^2(\Omega)}^2 + \frac{2\eta\Gamma(2-\alpha)}{(1-\lambda)t_n^{1-\alpha} + 2\gamma\Gamma(2-\alpha)} \sum_{j=1}^n \|f^{n-\frac{1}{2}}\|_{L^2(\Omega)}^2. \tag{4.11}$$

Using the Poincare inequality

$$\|U^n\|_{L^2(\Omega)}^2 \leq C_\Omega \|\nabla U^n\|_{L^2(\Omega)}^2,$$

we can rewrite the inequality (4.11) as

$$\|U^n\|_{L^2(\Omega)}^2 \leq \kappa \left\{ \beta \|U^0\|_{L^2(\Omega)}^2 + \frac{\eta\lambda\Gamma(2-\alpha)}{t_n^{1-\alpha}} \max_{1 \leq j \leq n} \|(U^{n-1})^3\|_{L^2(\Omega)}^2 + \frac{2\eta\Gamma(2-\alpha)}{(1-\lambda)t_n^{1-\alpha} + 2\gamma\Gamma(2-\alpha)} \max_{1 \leq j \leq n} \|f^{n-\frac{1}{2}}\|_{L^2(\Omega)}^2 \right\}, \tag{4.12}$$

where $\kappa = \frac{C_\Omega}{C_\Omega\beta + C_\Omega}$. By placing

$$M_1 = \frac{\kappa\eta\lambda\Gamma(2-\alpha)}{t_n^{1-\alpha}}, \text{ and } M_2 = \frac{2\kappa\eta\Gamma(2-\alpha)}{(1-\lambda)t_n^{1-\alpha} + 2\gamma\Gamma(2-\alpha)},$$

we get

$$\|U^n\|_{L^2(\Omega)}^2 \leq \kappa\beta \|U^0\|_{L^2(\Omega)}^2 + M_1 \max_{1 \leq j \leq n} \|(U^{n-1})^3\|_{L^2(\Omega)}^2 + M_2 \max_{1 \leq j \leq n} \|f^{n-\frac{1}{2}}\|_{L^2(\Omega)}^2, \tag{4.13}$$

and the proof is complete. □

5. NUMERICAL RESULTS

In this section, we use three examples in different dimensions to demonstrate the effectiveness of the method described in the previous sections. All algorithms are implemented in MATLAB software. To report the errors in numerical results, we use the L_2 and L_∞ errors. Also, we compute the numerical convergence order by the formula:

$$C - \text{order} = \frac{\log\left(\frac{e(i-1)}{e(i)}\right)}{\log 2}, \tag{5.1}$$

where $e(i)$ is the error corresponding to $t_i = i\eta$.

TEST PROBLEM 1

Consider the non-linear TFKG Equation (1.1) with coefficients $\zeta = \gamma = \beta = \lambda = 1$ and initial conditions

$$u(x, 0) = 0, \quad \frac{\partial u(x, 0)}{\partial t} = 0, \quad x \in \Omega = (0, 1), \tag{5.2}$$

and boundary conditions

$$u(0, t) = 0, \quad u(1, t) = 0. \tag{5.3}$$

For the exact solution

$$u(x, t) = t^2 x(x - 1), \tag{5.4}$$

we have the following right-hand side function

$$f(x, t) = \left(\frac{\Gamma(3)t^{2-\alpha}}{\Gamma(3-\alpha)} + 2t + t^2 \right) x(x - 1) - 2t^2 - t^6(x(x - 1))^3. \tag{5.5}$$



TABLE 1. The L_∞ and L_2 errors as functions of n_p at $T = 1$ (Test problem 1).

η	n_p	L_∞ -error		L_2 -error	
		$\alpha = 1.3$	$\alpha = 1.3$	$\alpha = 1.3$	$\alpha = 1.3$
1/256	4	$7.3213e - 06$	$8.2356e - 06$	$8.2356e - 06$	$8.2356e - 06$
1/1296	6	$1.2302e - 06$	$1.6585e - 06$	$1.6585e - 06$	$1.6585e - 06$
1/4096	8	$3.8032e - 07$	$5.9160e - 07$	$5.9160e - 07$	$5.9160e - 07$
1/10000	10	$1.5481e - 07$	$2.6906e - 07$	$2.6906e - 07$	$2.6906e - 07$
1/20736	12	$7.4507e - 08$	$1.4179e - 07$	$1.4179e - 07$	$1.4179e - 07$

TABLE 2. The L_∞ and L_2 errors for different final times with $n_p = 12$ and $\eta = 1/1728$ (Test problem 1).

T	L_∞ -error		L_2 -error	
	$\alpha = 1.5$	$\alpha = 1.3$	$\alpha = 1.5$	$\alpha = 1.3$
1	$6.5161e - 08$	$2.3105e - 08$	$1.3475e - 07$	$4.8841e - 08$
2	$8.4251e - 08$	$8.4936e - 08$	$1.7869e - 07$	$1.8008e - 07$
3	$1.9176e - 07$	$1.8903e - 07$	$4.0651e - 07$	$4.0095e - 07$
4	$3.3711e - 07$	$3.3542e - 07$	$7.1495e - 07$	$7.1149e - 07$
5	$5.2503e - 07$	$5.2372e - 07$	$1.1136e - 06$	$1.1109e - 06$

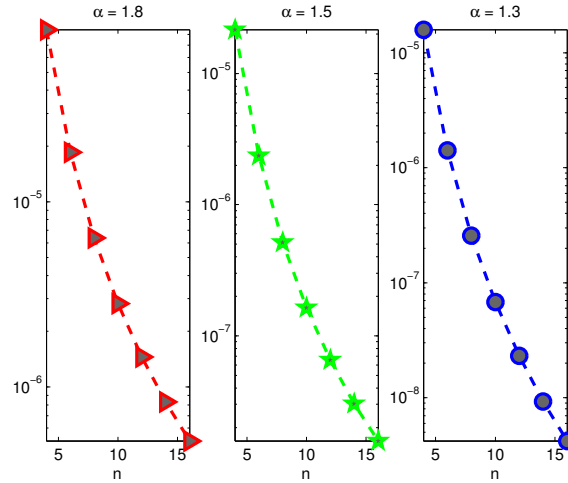
FIGURE 1. The L_∞ errors as functions of n_p for different values of α at $T = 1$ (Test problem 1).

Table 1 reports the L_∞ and L_2 errors of numerical solution as functions of n_p in final time $T = 1$. The results show that with the upward trend of n_p as well as decreasing the length of the time step, the obtained error has an exponential accuracy. Table 2 shows that the exponential accuracy for different final times remains, means that the presented method is desirable. Furthermore, Figure 1 shows the fast downward trend of the error for different α , which is one of the characteristics of the pseudo-spectral schemes.



TABLE 3. The L_∞ and L_2 errors as functions of n_p and C-order at $T = 1$ (Test problem 2).

	L_∞ -error	L_2 -error	C-order	CPU-Time
η	$\alpha = 1.3$	$\alpha = 1.3$		
1/10	$1.5789e - 04$	$5.9064e - 04$	—	0.1000
1/20	$4.0013e - 05$	$1.4931e - 04$	1.9804	0.1549
1/40	$1.0249e - 05$	$3.8055e - 05$	1.9650	0.2946
1/80	$2.6820e - 06$	$9.8671e - 06$	1.9341	0.5972
1/160	$7.2991e - 07$	$2.6421e - 06$	1.8775	1.3940
1/320	$2.1207e - 07$	$7.4796e - 07$	1.7832	1.8074
1/640	$6.7785e - 08$	$2.3073e - 07$	1.6455	1.9429

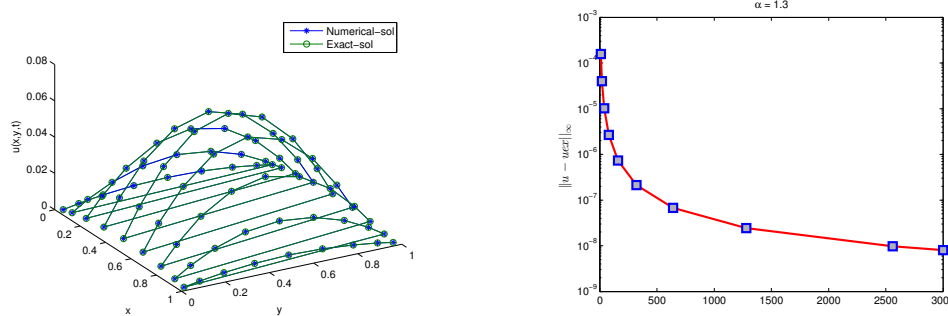


FIGURE 2. (left) Numerical and exact solution for $\alpha = 1.3$ at $T = 1$. (right) The L_∞ errors as functions of n_p for $\alpha = 1.3$ and different values of η at $T = 1$. (Test problem 2).

TEST PROBLEM 2

Now we consider the non-linear TFKG (1.1) in the two-dimensional domain $\Omega = (0, 1)^2$, with coefficients $\zeta = 1, \gamma = \beta = 0, \lambda = 1$ and homogeneous initial and boundary conditions. With the exact solution

$$u(x, y, t) = t^2 x(x - 1)y(y - 1), \tag{5.6}$$

the source term function is obtained as

$$f(x, y, t) = \frac{\Gamma(3)t^{2-\alpha}}{\Gamma(3-\alpha)} x(x-1)y(y-1) - 2t^2(x(x-1) + y(y-1)) - t^6(x(x-1)y(y-1))^3. \tag{5.7}$$

Table 3 reports the L_∞ and L_2 errors and the C-order of the numerical solution. As we expected, the presented method gives the desired spectral accuracy. According to the CPU-Times reported in Table 3, the execution speed of the method is good for different values of η . Figure 2 shows the numerical and exact solution for $\alpha = 1.3$ and the L_∞ errors as functions of n_p for different values of η at the final time $T = 1$. In Figure 3 we draw the numerical solution at different final times. Figure 4 shows the decrease of the maximum error by increasing the degree of the basic polynomials for different values of α at the final time $T = 1$.

TEST PROBLEM 3

For the three dimensional case, we consider the non-linear TFKG equation (1.1) with coefficients $\zeta = 1, \gamma = 1, \beta = 1, \lambda = 1$ on $\Omega = (0, 1)^3$. The initial and the boundary conditions are homogeneous, and the source term function can



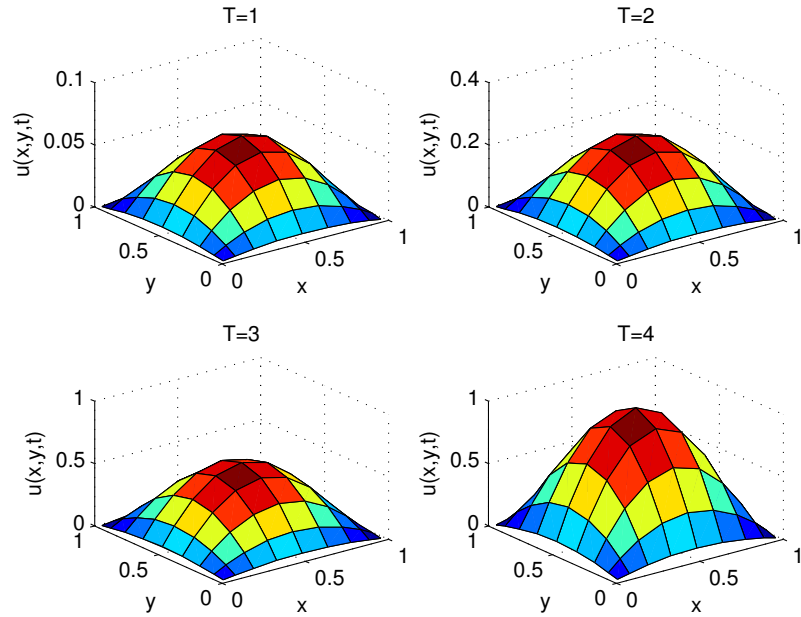


FIGURE 3. Numerical solution with $n_p = 10$, $\eta = \frac{1}{1280}$ and $\alpha = 1.5$ for the different values of the final time T (Test problem 2).

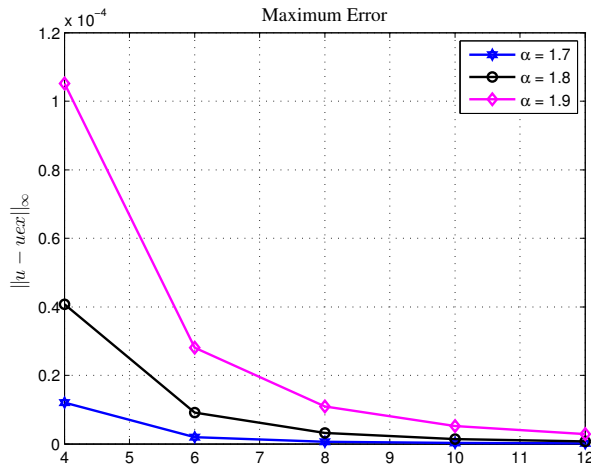


FIGURE 4. Maximum error vs. the basic polynomials degree for different values of α at $T = 1$ (Test problem 2).

be found from the exact solution

$$u(x, y, z, t) = t^2 \sin(\pi x) \sin(\pi y) \sin(\pi z). \tag{5.8}$$

The contents reported in Table 4 show that by shrinking η , the error is reduced, and we have the exponential accuracy. Considering that in this example, the three-dimensional state of the problem is considered, as the length



TABLE 4. The L_∞ and L_2 errors as functions of n_p and C-order at $T = 1$ (Test problem 3).

	L_∞ -error	L_2 -error	C-order	CPU-Time
η	$\alpha = 1.5$	$\alpha = 1.5$		
1/10	$6.1531e - 03$	$3.2105e - 02$	–	0.8125
1/20	$2.5994e - 03$	$1.2672e - 02$	1.2431	1.3110
1/40	$1.1776e - 03$	$5.4848e - 03$	1.1423	3.1645
1/80	$5.5792e - 04$	$2.5292e - 03$	1.0778	7.0981
1/160	$2.7119e - 04$	$1.2113e - 03$	1.0408	14.8132
1/320	$1.3365e - 04$	$5.9234e - 04$	1.0209	30.2491
1/640	$6.6334e - 05$	$2.9284e - 04$	1.0106	61.6015

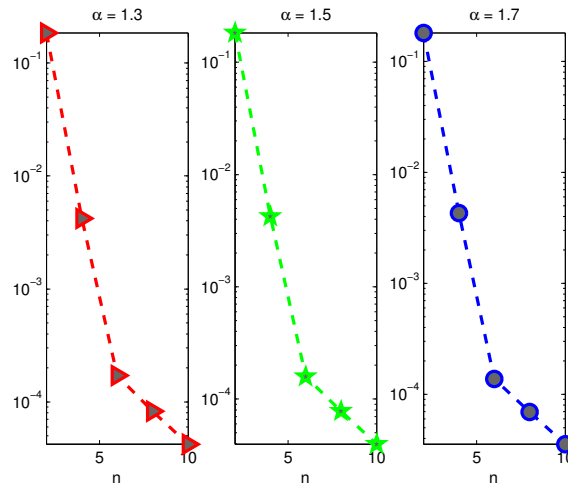


FIGURE 5. The L_∞ errors as functions of n_p for different values of α at $T = 1$ (Test problem 3).

of the time step increases, CPU-Time also increases, but this does not cause a difficulty in the process of numerical computation. Figure 5 shows the L_∞ errors as functions of n_p for different values of α at $T = 1$. We can see that when the degree of basic polynomials increases, the accuracy improves. Furthermore, in Figure 6, we plot the L_∞ and L_2 errors for $\alpha = 1.5$ and $n_p = 10$ for different time steps.

6. CONCLUSIONS

In this paper, we constructed a pseudo-spectral method based on the Lagrange polynomials for the solution of fractional PDEs containing linear and non-linear TFKG equations. To this end, we applied a finite difference scheme for discretizing the time derivatives and pseudo-spectral method for discretizing the spatial ones.

According to the results mentioned in the previous section, the errors of the method has a downward trend, and exponential accuracy is maintain in all dimensions for different α 's and for polynomials of various degrees. Also, we proved that the method is unconditionally stable.

In summary, our proposed method combines spectral accuracy, unique basis functions, demonstrated effectiveness, unconditional stability, and exponential accuracy. By explicitly highlighting these differences, we position our research as a valuable advancement in solving the non-linear time fractional equations.

These are our recommendations for future research directions:



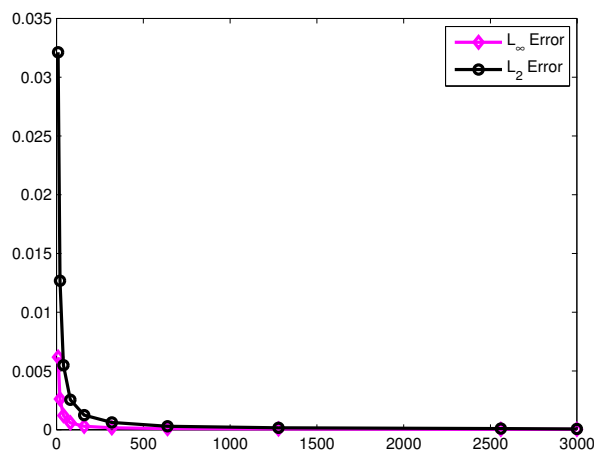


FIGURE 6. The L_∞ and L_2 errors for different values of η with $\alpha = 1.5$ at $T = 1$ (Test problem 3).

- Explore other types of time or spatial fractional PDEs or physical models that could benefit from the Pseudo-spectral Method.
- Investigate the applicability of the method to more complex geometries or boundary conditions.
- Explore hybrid approaches that combine the Pseudo-spectral Method with other numerical methods (e.g., finite element methods, finite difference methods).

ACKNOWLEDGMENT

The authors are grateful to the anonymous reviewers of this paper for their constructive comments and helpful suggestions, which have significantly improved the quality of the manuscript.

REFERENCES

- [1] D. Baleanu, J. A. T. Machado, and A. C. J. Luo, *Fractional dynamics and control*, Springer Science & Business Media, 2011.
- [2] A. Barone, F. Esposito, C. J. Magee, and A. C. Scott, *Theory and applications of the sine-Gordon equation*, La Rivista del Nuovo Cimento (1971-1977), 1(2) (1971), 227–267.
- [3] B. Batiha, M. S. M. Noorani, and I. Hashim, *Numerical solution of sine-Gordon equation by variational iteration method*, Phys. Lett. A, 370(5-6) (2007), 437–440.
- [4] J. P. Boyd, *Chebyshev and Fourier spectral methods*, Dover Publications, 2001.
- [5] C. Canuto and A. Quarteroni, *Spectral methods*, Wiley Online Library, 2006.
- [6] H. Chen, S. Lü, W. Chen, and others, *A fully discrete spectral method for the nonlinear time fractional Klein-Gordon equation*, Taiwanese J. Math., 21(1) (2017), 231–251.
- [7] K. Devendra, J. Singh, and D. Baleanu, *A hybrid computational approach for Klein-Gordon equations on Cantor sets*, Nonlinear Dyn., 87(1) (2017), 511–517.
- [8] K. Diethelm, *The analysis of fractional differential equations: An application-oriented exposition using differential operators of Caputo type*, Springer, 2010.
- [9] R. A. El-Nabulsi, *Generalized Klein-Gordon and Dirac equations from nonlocal kinetic approach*, Zeitschrift für Naturforschung A, 71(9) (2016), 817–821.
- [10] S. M. El-Sayed, *The decomposition method for studying the Klein-Gordon equation*, Chaos Solitons Fractals, 18(5) (2003), 1025–1030.



- [11] S. Esmaili, *Solving 2D time-fractional diffusion equations by a pseudospectral method and Mittag-Leffler function evaluation*, Math. Methods Appl. Sci., 40(6) (2017), 1838–1850.
- [12] H. R. Ghazizadeh, M. Maerefat, and A. Azimi, *Explicit and implicit finite difference schemes for fractional Cattaneo equation*, J. Comput. Phys., 229(19) (2010), 7042–7057.
- [13] A. K. Golmankhaneh, A. K. Golmankhaneh, and D. Baleanu, *On nonlinear fractional Klein-Gordon equation*, Signal Processing, 91(3) (2011), 446–451.
- [14] H. Gómez, I. Colominas, F. Navarrina, and M. Casteleiro, *A mathematical model and a numerical model for hyperbolic mass transport in compressible flows*, Heat and Mass Transfer, 45(2) (2008), 219–226.
- [15] R. M. Hafez, Y.H. Youssri, and A.G. Atta, *Jacobi rational operational approach for time-fractional sub-diffusion equation on a semi-infinite domain*, Contemp. Math., 4(4) (2023), 853–876.
- [16] R. Hilfer, *Applications of fractional calculus in physics*, World Scientific, 2000.
- [17] R. A. Horn and C. R. Johnson, *Matrix analysis*, Cambridge university press, 1990.
- [18] K. Hosseini, P. Mayeli, and R. Ansari, *Modified Kudryashov method for solving the conformable time-fractional Klein-Gordon equations with quadratic and cubic nonlinearities*, Optik (Stuttg.), 130 (2017), 737–742.
- [19] J. Klafter, S. C. Lim, and R. Metzler, *Fractional dynamics: recent advances*, World Scientific, 2012.
- [20] P. Lyu and S. Vong, *A linearized second-order scheme for nonlinear time fractional Klein-Gordon type equations*, Numer. Algorithms, 78 (2018), 485–511.
- [21] F. Mainardi, *Fractional calculus and waves in linear viscoelasticity: an introduction to mathematical models*, World Scientific, 2010.
- [22] A. Mohebbi, M. Abbaszadeh, and M. Dehghan, *High-order difference scheme for the solution of linear time fractional klein-gordon equations*, Numer. Methods Partial Differential Equations, 30(4) (2014), 1234–1253.
- [23] M. Moustafa, Y.H. Youssri, and A.G. Atta, *Explicit Chebyshev-Galerkin scheme for the time-fractional diffusion equation*, Internat. J. Modern Phys. C, 35(01) (2024), 2450002.
- [24] A. M. Nagy, *Numerical solution of time fractional nonlinear Klein-Gordon equation using Sinc-Chebyshev collocation method*, Appl. Math. Comput., 310 (2017), 139–148.
- [25] B. Nemati Saray, M. Lakestani, and C. Cattani, *Evaluation of mixed Crank-Nicolson scheme and Tau method for the solution of Klein-Gordon equation*, Appl. Math. Comput., 331 (2018), 169–181.
- [26] A. Ozkan and E. M. Ozkan, *Exact solutions of the space time-fractional Klein-Gordon equation with cubic nonlinearities using some methods*, Computational Methods for Differential Equations, 10(3) (2022), 674–685.
- [27] I. Podlubny, *Fractional differential equations: an introduction to fractional derivatives, fractional differential equations, to methods of their solution and some of their applications*, Academic press, Vol. 198, 1998.
- [28] Z.-Z. Sun and X. Wu, *A fully discrete difference scheme for a diffusion-wave system*, Appl. Numer. Math., 56(2) (2006), 193–209.
- [29] S. Taherkhani, I. Najafi Khalilsaraye, and B. Ghayebi, *A pseudospectral Sinc method for numerical investigation of the nonlinear time-fractional Klein-Gordon and sine-Gordon equations*, Computational Methods for Differential Equations, 11(2) (2023), 357–368.
- [30] L. N. Trefethen, *Spectral methods in MATLAB*, SIAM, 2000.
- [31] D. L. Turcotte, *Fractals and chaos in geology and geophysics*, Cambridge university press, 1997.
- [32] F. J. Valdes-Parada, J. A. Ochoa-Tapia, and J. Alvarez-Ramirez, *Effective medium equation for fractional Cattaneo's diffusion and heterogeneous reaction in disordered porous media*, Phys. A, 369(2) (2006), 318–328.
- [33] S. Vong and Z. Wang, *A compact difference scheme for a two dimensional fractional Klein-Gordon equation with Neumann boundary conditions*, J. Comput. Phys., 274 (2014), 268–282.
- [34] S. Vong and Z. Wang, *A high-order compact scheme for the nonlinear fractional Klein-Gordon equation*, Numer. Methods Partial Differential Equations, 31(3) (2015), 706–722.
- [35] A.-M. Wazwaz, *The tanh method: exact solutions of the sine-Gordon and the sinh-Gordon equations*, Appl. Math. Comput., 167(2) (2005), 1196–1210.
- [36] B. D. Welfert, *Generation of pseudospectral differentiation matrices I*, SIAM J. Numer. Anal., 34(4) (1997), 1640–1657.



- [37] F. Yin, J. Song, and F. Lu, *A coupled method of Laplace transform and Legendre wavelets for nonlinear Klein-Gordon equations*, Math. Methods Appl. Sci., 37(6) (2014), 781–792.
- [38] Y.H. Youssri, *Two Fibonacci operational matrix pseudo-spectral schemes for nonlinear fractional Klein-Gordon equation*, Internat. J. Modern Phys. C, 33(04) (2022), 2250049.
- [39] Y.H. Youssri and A.G. Atta, *Modal spectral Tchebyshev Petrov-Galerkin stratagem for the time-fractional nonlinear Burgers' equation*, Iran. j. numer. anal. optim., 14(1) (2024), 172–199.
- [40] Y.H. Youssri, M. I. Ismail, and A.G. Atta, *Chebyshev Petrov-Galerkin procedure for the time-fractional heat equation with nonlocal conditions*, Phys. Scr., 99(1) (2024), 015251.
- [41] E. Yusufoglu, *The variational iteration method for studying the Klein-Gordon equation*, Appl. Math. Lett., 21(7) (2008), 669–674.

Uncorrected Proof

